

Shearing of planar smectic C chevrons

N.J. Mottram^a and S.J. Elston

Department of Engineering Science, University of Oxford, Parks Road, Oxford, OX1 3PJ, UK

Received 28 December 1998 and Received in final form 8 April 1999

Abstract. We have theoretically investigated chevron formation in smectic C materials and the transformation of this chevron structure to a tilted layer structure as the cell is sheared. We find a series of transition temperatures at which the behaviour of the cell critically changes. As the cell is cooled from the smectic A phase past the first critical temperature there is a second order transition which forms two tilted layer states with *lower* energy than the smectic A bookshelf structure. Although these low energy tilted structures exist the bookshelf structure is the stable state for zero shear. However, upon further cooling this bookshelf structure becomes unstable to the formation of a chevron state. Now when the cell is sheared the chevron structure smoothly transforms into the tilted layer structure. As each further critical temperature is passed an additional *multiple* chevron solution is formed which although a high energy, unstable state may be observed transiently. For sufficiently low temperatures the transition from chevron to tilted layer becomes first order. This first order transition occurs as the chevron interface merges with the surface alignment region to form the tilted layer structure.

PACS. 61.30.Cz Theory and models of liquid crystal structure

1 Introduction

In recent years considerable effort has been devoted to the understanding of smectic C (S_C) and chiral smectic C ferroelectric liquid crystals (S_C^* or FLC). These materials are of great commercial interest due to the considerable potential for exploitation of ferroelectric liquid crystals in display devices. Key to the development of such devices is an understanding of the structures formed and the switching within surface stabilised homogeneously aligned cells. One of the most important features found within these cells is the chevron structure. This was first observed in surface stabilised ferroelectric liquid crystal (SSFLC) cells using X-ray diffraction in the S_C^* phase [1, 2], and later in thicker cells [3], and finally in the smectic A (S_A) phase [4]. The presence of two peaks in the diffraction pattern corresponded to equal and opposite layer tilts, $\pm\delta$, with a sharp transition between them.

This chevron structure is believed to form due to the mismatch between the prescribed S_A layer thickness at the cell surfaces and the layer thickness within the bulk of the cell which is determined by the smectic cone angle θ . This layer thickness matching condition can be satisfied by tilting the layers away from the cell surface normal. Recently Cagnon and Durand presented experimental evidence which supported the notion that at the cell surfaces the smectic layering is fixed in the smectic A state [5].

A number of theoretical models of the chevron structure have been developed in recent years [6–12]. The orig-

inal model of Clark *et al.* [6] assumed that, at the chevron interface, the smectic cone angle, θ , remained constant whilst the layer tilt angle, δ , was discontinuous. Subsequent models, which insist that the layer structure remains continuous throughout the cell, have allowed certain variables, such as the cone angle θ , the layer tilt angle δ and the azimuthal angle ϕ to vary at the chevron interface. In this paper we use a simple model, described below, of the chevron structure which assumes that there is no absolute layer compression and that the cell surfaces maintain smectic A ordering for all temperatures. In order to simplify the calculations we assume that the azimuthal angle is constant and that the director always lies in a plane perpendicular to the cell surfaces (see Fig. 1). We therefore restrict ourselves to considering *planar* chevrons, previously discussed by Vaupotič *et al.* [12], in which, in order to maintain a continuous layer tilt structure, the liquid crystal must become smectic A at the chevron interface. This simplified model is intended to show qualitatively the effect of shearing smectic chevrons. Clearly the chevrons contained within ferroelectric display devices are necessarily non-planar since the two possible chevron interface configurations produce the essential bistability of the device and whilst the regime of planar chevrons is small their behaviour under shear may be indicative of the behaviour of non-planar chevrons. It is also worth noting that, although in this paper we will concentrate on smectic C chevron behaviour due to their importance in display technology, the assumption that the director remains in the plane of the chevron implies that this model

^a e-mail: nigel.mottram@eng.ox.ac.uk

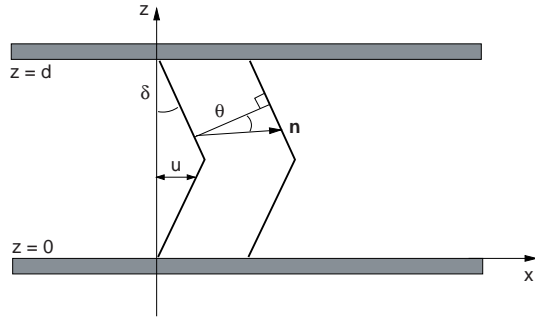


Fig. 1. The cell configuration (at zero shear) indicating the director \mathbf{n} which is contained within the xz -plane, the cone angle θ , the layer tilt angle δ and the layer displacement, u .

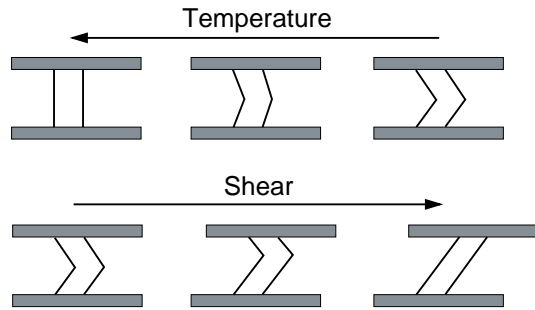


Fig. 2. The effects of temperature and shear. As the temperature decreases the chevron structures forms. With an applied shear this chevron structure transforms into a tilted layer.

will be particularly applicable to the formation of smectic A chevrons.

This paper is a continuation of our previous work [13] in which we considered the formation of the chevron structure as the material is cooled from the S_A state to the S_C state. In [13] we have shown that although a tilted layer structure may be energetically favourable in the smectic C phase, the chevron structure is stabilized due to the presence of surface ordering. This ordering forces the liquid crystal to be smectic A at the cell boundaries and thus the layer thickness is equal to the smectic A layer thickness which is assumed to be temperature independent. In this paper we consider in detail the change in the chevron structure *as the cell is sheared*. We find that the symmetric chevron structure transforms into the lower energy tilted chevron state through an asymmetric structure. For sufficiently large cone angles the transition from chevron to tilted layer is found to include a discontinuous jump from asymmetric chevron to tilted layer as the chevron tip is merged into the surface region (Fig. 2).

From this simple model we find a large number of complex structures including multiple chevrons. Although these high energy structures are unstable, they may be seen transiently as the chevron structure is formed from the smectic A bookshelf state.

2 Modelling

In our present model we assume that absolute layer compression or dilation requires too much energy to be likely to happen. Thus any change in layer thickness must be accompanied by changes in the cone angle, θ . We will also assume that the number of smectic layers within the cell is strictly preserved. There is no reorganisation of layers and no defects in the layering.

If we therefore start with a perfect bookshelf structure in the smectic A phase, a change in the cone angle in the bulk of the material will be accompanied by a tendency for the layers to tilt in order to retain the layer packing density wave. If the liquid crystal is strongly anchored at the surfaces this leads to the formation of a chevron consisting of regions of equal and opposite layer tilt. The chevron interface, between these two regions of opposite tilt, is assumed to be a localised bend of the layers as opposed to the discontinuous kink of the original model of Clark *et al.* [6]. This assumption directly implies the condition that the layer tilt, δ , is zero at the chevron interface. In order to preserve the layer packing density wave this also means that the liquid crystal will be in the smectic A phase at the chevron interface.

The structure of the chevron will be governed by a balance of forces due to deviations of the cone angle from its equilibrium bulk value and elastic forces due to distortions of the director field. For small cone angles the energy (per unit area) due to the former may be written in terms of a Landau-de Gennes expansion in even powers of θ (due to the symmetry, $\theta \leftrightarrow -\theta$),

$$F_{\text{LdeG}} = \int_0^d f_0 + \frac{a}{2}\theta^2 + \frac{b}{4}\theta^4 dz, \quad (1)$$

where $a = \alpha(T - T_{AC})$ and T_{AC} is the smectic A to C transition temperature. In (1) f_0 is the free energy in the undistorted smectic A phase *i.e.* when $\theta = 0$. Any constant energy term such as f_0 will not enter the minimization of the free energy and will subsequently be disregarded. This energy expression determines the bulk cone angle. Minimization of (1) leads to the solutions $\theta = 0, \pm\theta_e$ where

$$\theta_e = \sqrt{\frac{-a}{b}}. \quad (2)$$

Thus in an undistorted sample of smectic material the cone angle will be zero for temperatures above the transition temperature T_{AC} (*i.e.* $a > 0$) and non-zero for temperatures below T_{AC} (*i.e.* $a < 0$).

The energy due to distortions of the director, \mathbf{n} , can be written as the Frank nematic energy of distortions within a layer

$$F_{\text{nem}} = \int_0^d \frac{K}{2} \left((\nabla \cdot \mathbf{n})^2 + (\nabla \wedge \mathbf{n})^2 \right) dz, \quad (3)$$

where the one constant approximation has been used. If the director remains in the xz -plane the director \mathbf{n} may be written as (Fig. 1).

$$\mathbf{n} = (\cos(\delta - \theta), 0, \sin(\delta - \theta)). \quad (4)$$

In order to simplify the distortional energy we make certain key assumptions. We assume that the layer tilt angle, δ , and the smectic cone angle, θ , are small and that there is a direct relationship between them,

$$\delta = \nu\theta. \quad (5)$$

This relationship may describe rod-shaped liquid crystal molecules for which $\nu = 1$ or, the more realistic, ellipse-shaped liquid crystal molecules for which $\nu < 1$.

These approximations reduce the free energy to,

$$F_{\text{nem}} = \int_0^d \frac{K}{2} (1 - \nu)^2 \left(\frac{d\theta}{dz} \right)^2 dz. \quad (6)$$

The total free energy of the system is therefore

$$F = \int_0^d \frac{b}{4} (\theta^2 - \theta_e^2)^2 + \frac{K'}{2} \left(\frac{d\theta}{dz} \right)^2 dz, \quad (7)$$

where $K' = K(1 - \nu)^2$.

In order to find the equilibrium configuration, the free energy must be minimized subject to certain constraints at the cell surfaces.

We wish to include a parameter which measures the total amount of shear between the two surfaces. We assume that the lower surface, $z = 0$, is fixed whereas the upper surface, $z = d$, is sheared by an amount τ . If, as in Figure 1, we define the layer displacement, $u(z)$, as the displacement away from the bookshelf geometry then the amount of shear is $\tau = u(d) - u(0)$. Using the fact that the layer tilt angle is given by $\tan \delta = du/dz$ we may write,

$$u(d) - u(0) = \int_0^d \frac{du}{dz} dz = \int_0^d \tan \delta dz. \quad (8)$$

The lower surface is fixed so $u(0) = 0$ and the layer tilt angle is small and related to θ . Thus this expression becomes,

$$\tau = \int_0^d \nu\theta dz. \quad (9)$$

Hence the total shear is related to the chevron configuration given by $\theta(z)$.

The other boundary conditions are related to the induced ordering at the cell surfaces. We assume that the liquid crystal is strongly anchored in the direction of the layer normal at the cell surfaces. This implies that the cone angle, θ , is equal to the layer tilt angle, δ , there. From (5), assuming that $\nu \neq 1$, this will only occur in the smectic *A* phase *i.e.* when $\theta = 0$. The boundary conditions are therefore

$$\theta = 0 \text{ on } z = 0, d. \quad (10)$$

We now have the full problem. We must determine the chevron structure, $\theta(z)$, which minimizes the free energy (7) subject to the constraints (9) and (10).

By incorporating the constraint (9) into the energy minimization with the use a Lagrange multiplier λ , this problem is equivalent to minimizing the functional

$$F = \int_0^d \frac{b}{4} (\theta^2 - \theta_e^2)^2 + \frac{K'}{2} \left(\frac{d\theta}{dz} \right)^2 + \lambda \left(\nu\theta - \frac{\tau}{d} \right) dz, \quad (11)$$

with respect to θ and λ subject to the boundary conditions (10).

Minimizing with respect to θ leads to the Euler-Lagrange equation,

$$0 = K' \frac{d^2\theta}{dz^2} - b\theta (\theta^2 - \theta_e^2) - \nu\lambda. \quad (12)$$

It is this equation subject to the constraint (9) that we will solve numerically. The system may be nondimensionalised thus

$$\frac{d^2\theta}{dZ^2} - B\theta (\theta^2 - \theta_e^2) - \Lambda = 0, \quad (13)$$

$$\int_0^1 \theta dZ = \eta, \quad (14)$$

$$\theta = 0 \text{ on } Z = 0, 1. \quad (15)$$

where $B = bd^2/K'$, $Z = z/d$ and $\eta = \tau/(d\nu)$.

We therefore have three parameters, B , the ratio of energy terms associated with changes in the cone angle and distortions of the director, θ_e , the equilibrium bulk cone angle and η , the normalised shear. If we assume the material constant B is largely independent of temperature then our two control parameters will be θ_e and η , changes of which correspond to changes in temperature and shear respectively.

As mentioned previously this model may also be applied to smectic *A* chevron behaviour. If, in equations (13–15), we replace θ by the layer tilt δ then the system can be used to model shearing of smectic *A* materials with temperature dependent layer thickness. In the zero shear case this model of smectic *A* chevrons reduces to the model of Limat and Prost [14].

In the next section we are able to investigate analytically the stability of the bookshelf structure. Further analytic progress is hindered by the complexity of these nonlinear coupled integral and differential equations. We therefore use the numerical continuation package AUTO97 [15,16] to solve equation (13) subject to the constraint (14) and the boundary conditions (15).

2.1 Stability of the bookshelf structure

In this section we will examine the stability of the bookshelf structure as the temperature, or equivalently the equilibrium cone angle, is varied. Introducing a general perturbation of the bookshelf structure the system is stable or unstable if this perturbation respectively increases or decreases the free energy. Since the free energy (7)

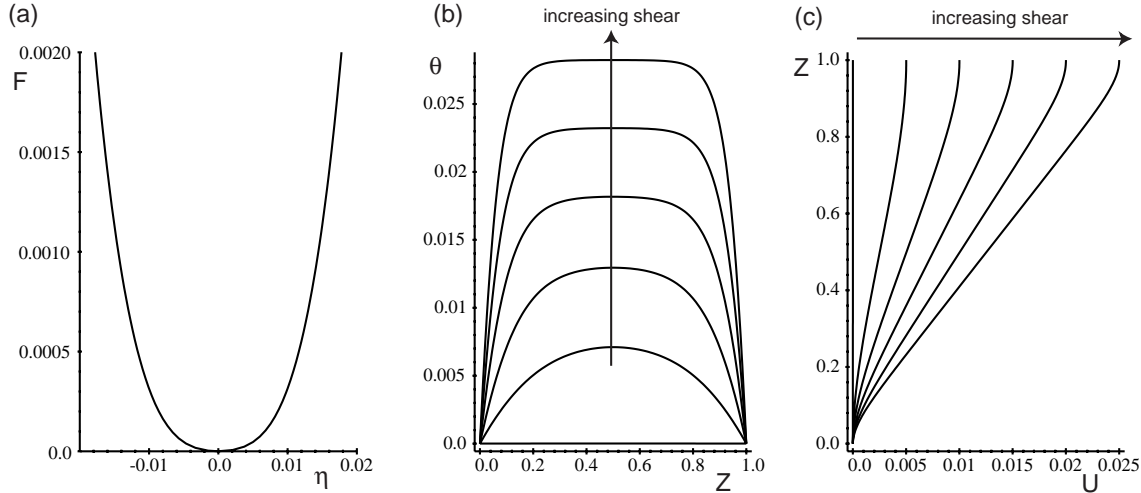


Fig. 3. Numerical solutions at the Sm_A - Sm_C phase transition ($\theta_e = 0.0$). (a) The free energy F , versus nondimensionalised shear η . (b) The cone angle θ and (c) the nondimensionalised layer displacement U through the cell for shear values $\eta = 0.0, 0.005, 0.01, 0.015, 0.02, 0.025$. At the cell surfaces ($Z = 0, 1$) the cone angle fixed at zero so that the material is smectic A whereas the interior of the cell is smectic C where the cone angle increases with shear.

does not contain information about the surface anchoring we choose perturbations of the system which satisfy the boundary conditions.

The smectic A bookshelf structure is described by $\theta(z) = 0$. It is a stationary point of the free energy (7) for all values of θ_e and satisfies the shear constraint for $\eta = 0$. As indicated above, stability of the bookshelf may be investigated by considering individual modes of instability,

$$\theta = \epsilon \sin(i\pi Z), \quad (16)$$

where $i = 1, 2, 3, \dots$. This form of θ automatically satisfies the boundary conditions (15) and for odd values of i the total shear η is non-zero whilst for even i , $\eta = 0$. Therefore if the bookshelf structure is unstable with respect to the above perturbation (16) it is unstable to a tilted layer if i is odd and a chevron structure if i is even.

Substituting (16) into the free energy (7) gives

$$F = \frac{K'}{d} \left(\frac{B\theta_e^4}{4} + \frac{\epsilon^2}{4} (\pi^2 i^2 - B\theta_e^2) + O(\epsilon^4) \right). \quad (17)$$

If the coefficient of ϵ^2 is positive the bookshelf structure is stable to such a perturbation whilst if it is negative the bookshelf is unstable. Hence for values of the equilibrium cone angle θ_e less than or greater than the critical value

$$\theta_e^{(i)} = \frac{i\pi}{\sqrt{B}}, \quad (18)$$

the bookshelf structure is stable or unstable respectively, to the i th mode. Using the typical parameter values [17], $K = 10^{-11}$ N, $\alpha = 1.7 \times 10^2$ Nm^{-2}/K , $b = 4.1 \times 10^4$ Nm^{-2} , $\nu = 0.85$ and $d = 10^{-6}$ m we obtain $B = 1.822 \times 10^5$ and $\theta_e^{(i)} = 0.00736i$ rads ($= 0.42169i^\circ$).

The first mode to become unstable is $i = 1$ at $\theta_e^{(1)} = 0.00736$ which is a tilted layer. Therefore for temperatures

above $T^{(1)} = T_{AC} - 0.013^\circ\text{C}$, shearing the cell induces a *stressed* tilted layer structure and the free energy of the system increases. Below $T^{(1)}$ the bookshelf structure is a stressed state and shearing the cell will *decrease* the free energy. The global minimum energy structure is then a tilted layer with a specific value of the layer tilt, δ .

The next mode to become unstable is $i = 2$ at $\theta_e^{(2)} = 0.01472$ which is a chevron. Thus below $T^{(2)} = T_{AC} - 0.052^\circ\text{C}$ the stable zero shear state is now the chevron structure. The bookshelf structure is an unstable, high energy state. Higher modes represent more complex structures associated with multiple chevrons and chevron/tilted layer combinations and may be seen in more detail in the subsequent numerical solutions.

The above analysis is only valid close to the critical values of θ_e . In order to investigate the layer configurations at all temperatures we will now numerically solve the governing equations.

2.2 Numerical solutions

Using the numerical continuation package AUTO97 we are able to calculate solutions of equations (13–15) as certain parameters are varied. Figures 3–8 show the numerical results as the nondimensionalised shear, η , is varied for various values of θ_e using the parameter value $B = 1.822 \times 10^5$ found in the previous section.

For each value of θ_e the free energy of the system, F , is plotted as η varies (*e.g.* Fig. 3a). At each value of θ_e we have also plotted the cone angle $\theta(Z)$ and the nondimensionalised layer displacement $U(Z) = u(Z)/(d\nu)$ for various values of η on the solution branch (*e.g.* Figs. 3b and 3c). In these figures solid and dashed lines indicate stable and unstable solutions respectively.

When $\theta_e = 0$ (*i.e.* at the transition temperature $T = T_{AC}$) the bookshelf configuration is stable and is

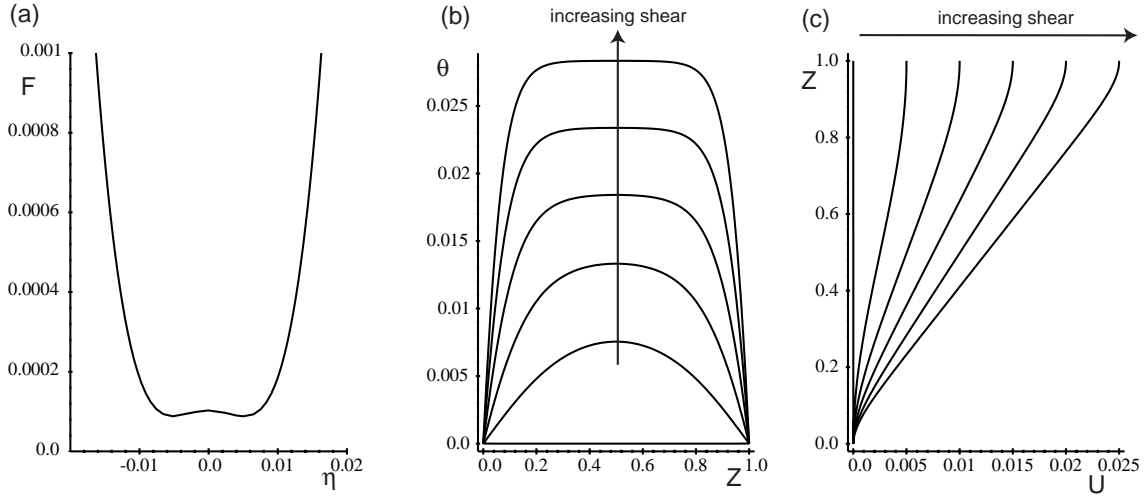


Fig. 4. Numerical solutions for $\theta_e = 0.01$. (a) The free energy F , versus nondimensionalised shear η . (b) The cone angle θ and (c) the nondimensionalised layer displacement U through the cell for shear values $\eta = 0.0, 0.005, 0.01, 0.015, 0.02, 0.025$. As in Figure 3 the material is smectic A at the cell surfaces and smectic C in the interior.

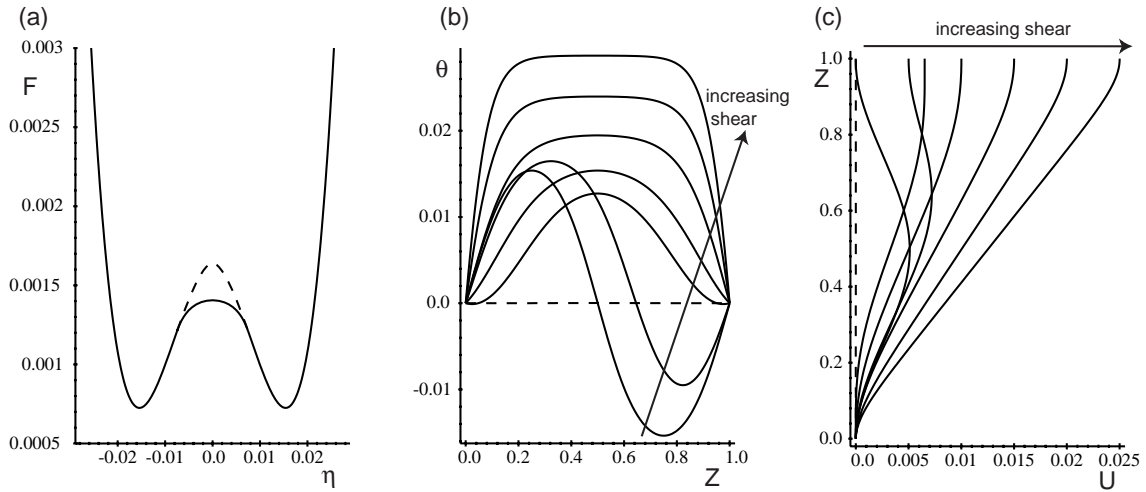


Fig. 5. Numerical solutions for $\theta_e = 0.02$. (a) The free energy F , versus shear η . (b) The cone angle θ and (c) the layer displacement U through the cell. For $\eta = 0$ the unstable bookshelf (dashed line) and stable chevron structures exist. As η increases the chevron transforms to a tilted layer through an asymmetric chevron structure.

the minimum energy configuration with respect to changes in the value of the shear η (Fig. 3a). If the cell is sheared the free energy increases and the bookshelf continuously transforms into a tilted layer (Fig. 3c). In order to preserve the layer density wave the layer tilting is accompanied by an increase in the value of the cone angle in the cell (Fig. 3b). The smectic A ordering at the surface leads to boundary layers at $z = 0$ and d where the layer tilt induced by shear realigns to ensure that $\delta = 0$ (and $\theta = 0$) at the surface. In this tilted layer situation it is only at the surfaces that the material is smectic A whereas the interior of the cell is smectic C .

As θ_e increases past the first critical value $\theta_e^{(1)} = 0.00736$ found in the previous section the bookshelf structure is no longer the minimum energy

configuration for all shear values (Fig. 4a). There now exist two symmetric states with non-zero values of η which are the global energy minimizers corresponding to tilted layers. It should be noted that for $\eta = 0$ the bookshelf structure *is* the stable configuration. It is only if the cell is sheared that it reaches its minimum energy configuration. The $\theta(Z)$ and $U(Z)$ plots (Figs. 4b and 4c) show that, as for $\theta_e < \theta_e^{(1)}$, the bookshelf structure continuously transforms into a tilted layer structure as η increases.

Figure 5 shows typical solutions for $\theta_e^{(2)} < \theta_e < \theta_e^{(3)}$ ($0.01472 < \theta_e < 0.02208$). The bookshelf is now *not* stable. As θ_e increases past $\theta_e^{(2)}$ a second solution branch forms (at $\eta = 0$) with a lower energy than the bookshelf branch. This is the (single) chevron solution branch. Thus

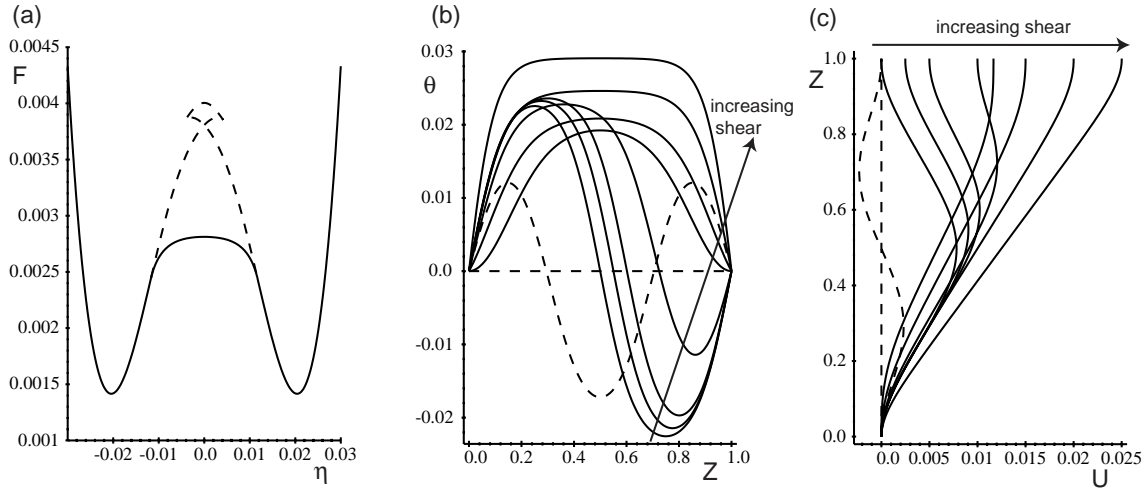


Fig. 6. Numerical solutions for $\theta_e = 0.025$. (a) The free energy F , versus shear η . (b) The cone angle θ and (c) the layer displacement U through the cell. At zero shear ($\eta = 0$) there are now three solutions, the high energy, unstable bookshelf, the intermediate energy, unstable double chevron characterised by *two* chevron interfaces within the cell (both dashed lines) and the low energy, stable chevron.

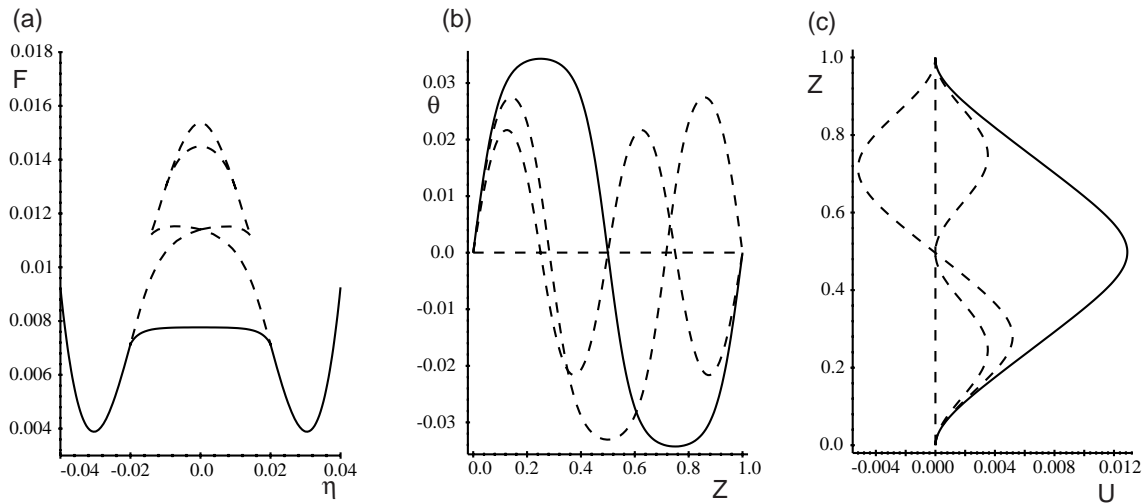


Fig. 7. Numerical solutions for $\theta_e = 0.035$. (a) The free energy F , versus shear η . (b) The cone angle θ and (c) the layer displacement U through the cell for $\eta = 0$ only. There now exists four zero shear solutions, the high energy, unstable bookshelf, the intermediate energy, unstable double and triple chevron structures (dashed lines) and the low energy, stable chevron.

in Figure 5a the lower energy, stable branch at $\eta = 0$ corresponds to the chevron solution whilst the higher energy, unstable branch corresponds to the bookshelf solution. Figures 5b and 5c show the unstable bookshelf solution ($\theta(Z) = 0$, $U(Z) = 0$), the stable chevron solution and how this chevron is continuously transformed to the tilted layer as η is increased. We see that the chevron interface, which lies in the centre of the cell when $\eta = 0$, moves towards the upper cell surface forming an asymmetric chevron as the cell is sheared and eventually combines with the surface boundary layer forming the tilted layer. The point where the bookshelf/tilted layer branch meets the chevron branch is the point where the chevron interface region meets the surface boundary layer region (at approximately $\eta = 0.0075$ in Fig. 5a).

For $\theta_e^{(3)} < \theta_e < \theta_e^{(4)}$ ($0.02208 < \theta_e < 0.02944$) two limit points form from the point $\eta = 0$ (Fig. 6a). Between these limit points the solution is now a tilted layer/chevron combined structure. The stable branch is essentially the same chevron structure as for lower values of θ_e , and again this structure continuously transforms into a tilted layer as η increases. Figures 6b and 6c show the solutions for $\eta = 0$ and the solutions along the stable branch. For zero shear ($\eta = 0$) the solutions are now the high energy, unstable bookshelf structure, an intermediate energy, unstable *double* chevron structure which contains two chevron interfaces and the low energy, stable chevron structure.

As θ_e increases past $\theta_e^{(4)}$ (Fig. 7) two bifurcation points emerge from $\eta = 0$ between which there exists a new

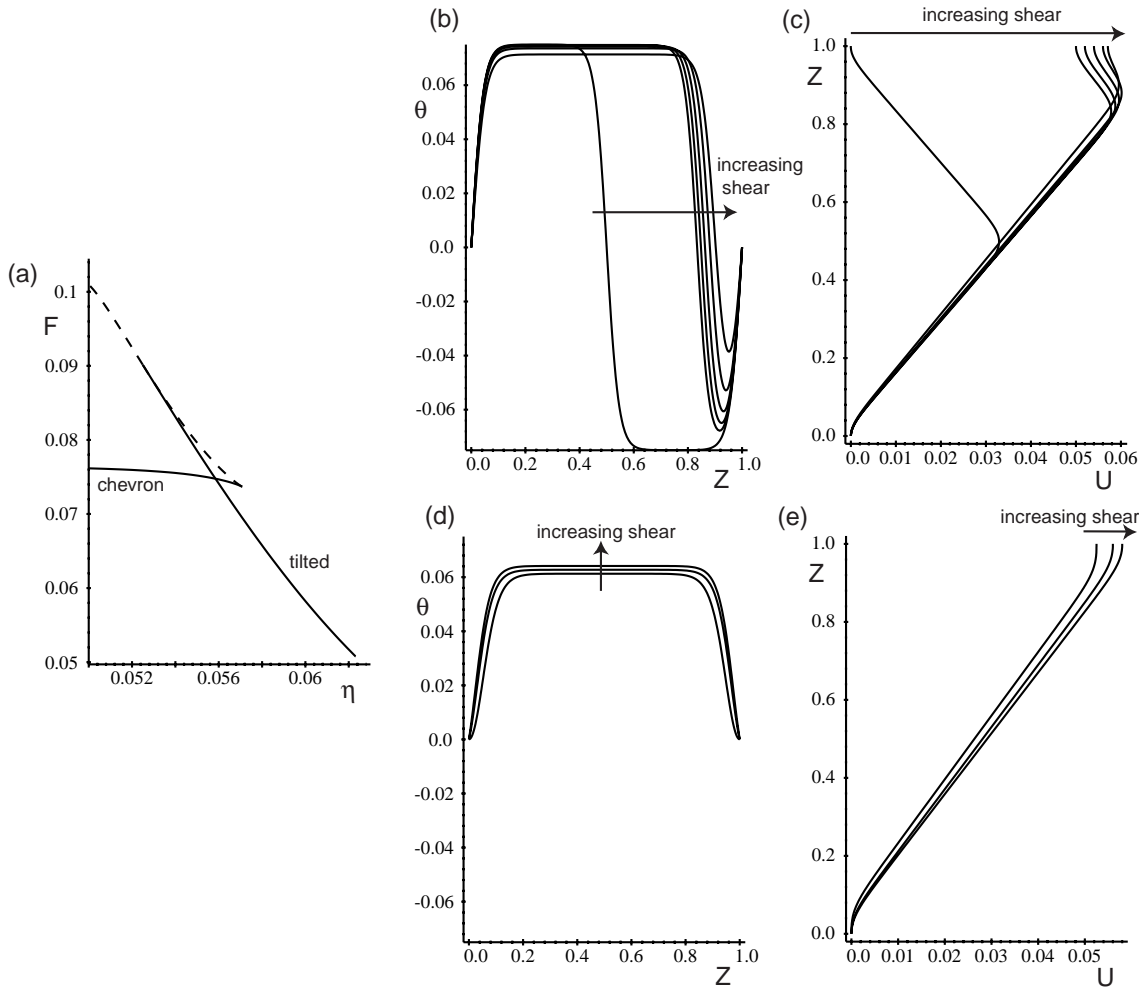


Fig. 8. Numerical solutions for $\theta_e = 0.075$. (a) The free energy F , versus shear η near to the transition from single chevron to tilted layer. (b) The cone angle θ and (c) the layer displacement U on the single chevron branch. (d) The cone angle θ and (d) the layer displacement U on the tilted layer branch.

solution branch. The zero shear solutions are shown in Figures 7b and 7c. The unstable bookshelf, double chevron and the stable chevron are now joined by a *triple* chevron which contains three chevron interfaces. The behaviour of the stable branch is as for lower values of θ_e . The chevron structure smoothly transforms to a tilted layer.

For larger values of θ_e the structure above the stable chevron branch becomes increasingly more complicated as the process described above repeats. At the odd critical points $\theta_e = \theta_e^{(3)}, \theta_e^{(5)} \dots$ two limit points form at $\eta = 0$ whilst at the even critical points $\theta_e = \theta_e^{(4)}, \theta_e^{(6)} \dots$ two bifurcation points form at $\eta = 0$ connected by a lower energy branch on which the solution is a multiple chevron. All of these solutions branches are unstable branches.

In all the above cases the transition from the stable single chevron structure to the tilted layer has been continuous as the shear, η , increases. However for large enough values of θ_e we find that this is not the case. Figure 8a shows, in detail, the region where the unstable branch joins the stable branch for $\theta_e = 0.075$. There now exist multiple solutions for a range of η values. The solu-

tions on the two stable branches are shown in Figures 8b–8e. As the chevron interface meets the surface boundary layer a first order transition occurs between an asymmetric chevron and a tilted layer. Although the energy difference between the two branches is never large in Figure 8a, for lower temperatures (and therefore larger values of θ_e) the energy difference increases. The relaxation process from the high energy chevron branch to the low energy tilted layer branch (or *vice versa*) may then be experimentally observable.

3 Discussion

We have investigated chevron formation in smectic C materials as the temperature is decreased below the transition temperature T_{AC} and the formation of a tilted layer structure as the cell is sheared. We find that below a critical value of the bulk cone angle, $\theta_e^{(2)} = 0.01472$ (or equivalently below the temperature $T^{(2)} = T_{AC} - 0.052$ °C), the bookshelf structure is stable for zero shear. It is only for

cone angles greater than $\theta_e^{(2)}$ that the chevron structure forms. For larger values of θ_e whilst the chevron structure is still the only stable solution for $\eta = 0$ there may be a large array of unstable solutions, corresponding to multiple chevrons, at higher energies. These solutions may be important if the liquid crystal is quickly cooled from the smectic *A* phase into the smectic *C* phase. Starting from the unstable, bookshelf structure the system would transform to the stable, single chevron structure. As we see from Figure 7 this may involve moving through various intermediate, multiple chevron structures whilst maintaining zero shear. In a dynamic model of the system these intermediate structures may be seen transiently [18].

For non-zero shear a tilted layer structure is the global energy minimizer for cone angles greater than $\theta_e^{(1)} = 0.00736$ (or temperatures lower than $T^{(1)} = T_{AC} - 0.013$ °C). The smectic liquid crystal then exerts a shear force on the upper surface. If the upper surface was free to move it would therefore move in order that tilted layers were formed within the cell.

For sufficiently large cone angles this transition from chevron to tilted layer goes through a first order transition. Assuming that the cell is sufficiently defect free, the system will follow the higher energy, chevron branch (Figs. 8b and 8c) as long as it exists and then relax to the lower energy, tilted layer branch.

This surface shear force, exerted by the liquid crystal, and the first order transition are expected to be apparent if an equivalent experiment to that of Cagnon and Durand [5] was carried out on smectic *C* materials.

The authors would like to acknowledge the financial support of Sharp Laboratories of Europe (SLE) Ltd and the EPSRC.

References

1. N.A. Clark, S.T. Lagerwall, *Proc. 6th Int. Display Research Conf., Tokyo, Japan* **456** (1986).
2. T.P. Rieker, N.A. Clark, G.S. Smith, D.S. Parmer, E.B. Sirota, R. Safinya, *Phys. Rev. Lett.* **59**, 2658 (1987).
3. Y. Ouchi, J. Lee, H. Takezoe, A. Fukuda, K. Kondo, T. Kitamura, A. Mukoh, *Jap. J. Appl. Phys. Lett.* **27**, 725 (1988).
4. Y. Takanishi, Y. Ouchi, H. Takezoe, A. Fukuda, *Jap. J. Appl. Phys.* **28**, 487 (1989).
5. M. Cagnon, G. Durand, *Phys. Rev. Lett.* **70**, 2742 (1993).
6. N.A. Clark, T.P. Rieker, *Phys. Rev. A* **37**, 1053 (1988).
7. M. Nakagawa, *Displays* **11**, 67 (1990).
8. S. Mukai, M. Nakagawa, *J. Phys. Soc. Jap.* **61**, 112 (1992).
9. A. De Meyere, H. Pauwels, E. De Ley, *Liq. Cryst.* **14**, 1269 (1993).
10. L. Limat, *J. Phys. II France* **5**, 803 (1995).
11. N. Vaupotič, S. Kralj, M. Čopič, T.J. Sluckin, *Phys. Rev. E* **54**, 3783 (1996).
12. N. Vaupotič, M. Čopič, T.J. Sluckin, *Phys. Rev. E* **57**, 5651 (1998).
13. N. Ul Islam, N.J. Mottram, S.J. Elston, *Liq. Cryst.* **26**, 1059 (1999).
14. L. Limat, J. Prost, *Liq. Cryst.* **13**, 101 (1993).
15. E.J. Doedel, *Congr. Numer.* **30**, 265 (1981).
16. E.J. Doedel, X.J. Wang, Center for Research on Parallel Computing, California Institute of Technology, Technical Report No. CRPC-95-2, (1995).
17. L. Ruan, J.R. Sambles, M.J. Towler, *Liq. Cryst.* **18**, 81 (1995).
18. T.J. Sluckin, presented at *Workshop on the Mathematical Modelling and Applications for Liquid Crystals in Confined Geometries, Cortona, Italy* (1998).